(Received 13 June 2024, Accepted 29 July 2024, Scheduled 12 August 2024)

DOA Estimation Based on Distributed Array Optimization in Impulsive Noise

Xiang Sha[1,*], Guolong Cui[1], and Yanan Du[2]

[1] *School of Information and Communication Engineering, University of Electronic Science and Technology of China, Chengdu 611731, China*
[2] *The 38th Research Institute of China Electronics Technology Group Corporation, Hefei 230088, China*

ABSTRACT: Aiming at the current distributed array subarray optimization design and DOA estimation problem, a robust and effective distributed array subarray optimization method is proposed, and a discrete quantum electromagnetic field optimization algorithm is designed to quickly solve the resulting objective function to obtain the optimal subarray structure. Then, based on this array structure, the infinite-norm exponential kernel maximum likelihood method is utilized for direction of arrival (DOA) estimation. The simulation results show that the proposed method can still be effective in the case of impulsive noise, small snapshots, and low signal-to-noise ratio, which further verifies that the proposed method can obtain a better subarray layout and superior DOA estimates.

1. INTRODUCTION

Distributed array is an innovative array configuration that can be considered as multiple uniform sub-arrays spatially dispersed [1]. Its flexible array layout and unique sub-array structure endow it with greater reconfigurability, enhanced mobility, and improved resilience against attacks. Distributed cooperative detection is a crucial method for enhancing spatial resolution capabilities and facilitating precise target localization, where direction of arrival (DOA) estimation plays a pivotal role [2–6]. Consequently, exploring the optimal arrangement of distributed sub-arrays and conducting DOA estimation research based on distributed arrays represent significant research topics in the field of array signal processing.

Currently, distributed arrays predominantly employ greedy algorithms, threshold-based algorithms, and convex optimization sparse recovery methods for estimating the DOAs of incoming signals [7]. Representative greedy sparse recovery algorithms include the orthogonal matching pursuit (OMP) method [8] and compressive sampling matching pursuit (CoSaMP) method [9]. The core idea of these algorithms is to iteratively select the DOA corresponding to the target echo that best matches the residual received signal. The advantages of these algorithms lie in their low computational complexity and broad applicability. However, their drawback is that each DOA estimation relies on the accuracy of the previous estimations, making them susceptible to noise. Threshold-based sparse recovery algorithms are represented by the iterative hard thresholding (IHT) algorithm [10] and hard thresholding pursuit algorithm [11]. Their core concept involves designing a threshold to determine the descent direction of the cost function for the ℓ-norm minimization sparse optimization problem. Compared to greedy methods, threshold-based methods better represent the iterative direction of sparse characteristics, but solving the ℓ-norm minimization problem is inherently a non-convex optimization problem, making it challenging to ensure iterative convergence speed and global optimality. Convex optimization sparse recovery algorithms are exemplified by the basis pursuit (BP) algorithm [12], iterative soft thresholding (IST) algorithm [13], and fast iterative shrinkage-thresholding algorithm (FISTA) [14]. The central idea here is to relax the non-convex ℓ-norm optimization problem into a convex optimization problem of ℓ_1-norm minimization, providing faster convergence speeds and guarantee global optimal performance. It has been demonstrated that these methods can achieve precise sparse solutions when the observation matrix meets specific conditions, such as the mutual coherence criterion [15] and restricted isometry property (RIP) [16].

Most of the aforementioned methods operate under the premise of uniformly distributed subarrays, without exploring the optimal subarray arrangement structure. Consequently, they do not fully leverage the advantages of distributed array concepts. Furthermore, the DOA estimation methods for distributed arrays often fail to achieve superior direction-finding performance in complex environments such as impulsive noise, low generalized signal-to-noise ratio (GSNR), and small snapshot scenarios, indicating significant room for improvement.

To achieve more accurate estimation under impulsive noise, we utilize the infinite norm exponential kernel (INEK) [17] to suppress impulsive noise and then minimize the root mean square error (RMSE) of the DOA estimation. The corresponding distributed array layout structure represents the optimal structure. However, this approach incurs high computational costs. To address this drawback, we draw inspiration from electromagnetic field optimization mechanisms [18] and quan-

* Corresponding author: Xiang Sha (202012012342@std.uestc.edu.cn).

tum computing and design a discrete quantum electromagnetic field optimization (DQEFO) algorithm. Finally, we employ the INEK-based maximum likelihood (ML) method for DOA estimation [17]. Simulations comparing our method with traditional algorithms in various scenarios demonstrate the superiority of our approach. The main contributions are as follows:

1. A distributed array optimization scheme based on INEK was designed, achieving superior array layout under impulsive noise conditions, which not only mitigates the severe performance degradation of distributed arrays under certain extreme conditions but also enhances the DOA estimation performance of distributed array systems.

2. By leveraging quantum encoding and quantum evolution mechanisms to address the limitations of electromagnetic field optimization in discrete optimization problems, the designed DQEFO algorithm effectively searches for the optimal subarray layout structure, reducing the computational complexity and ensuring the superiority of the resultant subarray layout.

The following is the rest of this work. Section 2 shows the distributed array optimization model. Section 3 shows DOA estimation using DQEFO-based distributed array optimization. Section 4 conducts the simulations, and Section 5 concludes this paper.

2. DISTRIBUTED ARRAY OPTIMIZATION MODEL

First, we arrange N narrowband far-field auxiliary sources with precisely known azimuths in space, with a wavelength of λ. The azimuth angle of the $\hat{n}$th source is $\theta_{\hat{n}}$, $\hat{n} = 1, 2, \cdots, N$ $-\pi/2 \leq \theta_{\hat{n}} \leq \pi/2$. The number of array elements in the distributed system is M, with each subarray containing G elements. The subarrays are arranged in a uniform linear array (ULA) configuration, with an element spacing of $\hat{d}$. The number of subarrays is Z, $M = G \times Z$. The spatial arrangement of the subarrays follows a one-dimensional layout, as depicted in Fig. 1, with the spacing between subarrays d_h being an integer multiple of the element spacing $\hat{d}$, i.e.,

$$d_h = \bar{s}_h \cdot \hat{d} \tag{1}$$

where $\bar{s}_h \in \mathbb{Z}$, $h = 1, \cdots, Z-1$. Therefore, the spacing vector between subarrays $\mathbf{d} = [d_1, d_2, \cdots, d_{Z-1}]$ represents the

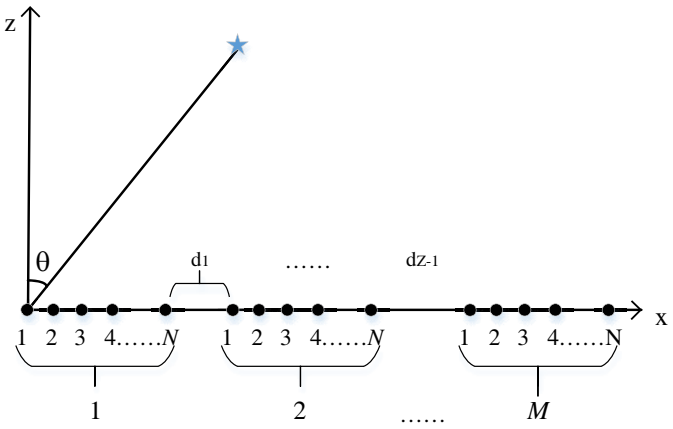

FIGURE 1. Schematic diagram of distributed array subarray layout optimization.

layout structure information of the distributed array to be optimized. Given that the subarray spacing is an integer multiple of the element spacing $\hat{d}$, the optimization parameters can be further simplified to obtain $\bar{\mathbf{s}} = [\bar{s}_1, \bar{s}_2, \cdots, \bar{s}_{Z-1}]$.

The RMSE of source estimation in distributed arrays can be obtained through the following process. First, given an arbitrary layout $\bar{\mathbf{s}}$ for the distributed array, place the array in a spatial environment configured with auxiliary sources and corresponding noise. The mathematical model for the lth snapshot of the received data by the array is

$$\mathbf{B}(l) = \mathbf{A}(\theta)\mathbf{s}(l) + \mathbf{n}(l) \tag{2}$$

where $\mathbf{B}(l) = [B_1(l), B_2(l), \ldots, B_M(l)]^T$ represents the received signal vector; $\mathbf{s}(l)$ is the source signal vector; $\mathbf{n}(l)$ denotes the impulsive noise vector, which follows the SαS distribution described by scale γ and characteristic exponent α; $\mathbf{A}(\boldsymbol{\theta}) = [\mathbf{a}(\theta_1), \mathbf{a}(\theta_2), \ldots, \mathbf{a}(\theta_N)]$ is the array manifold matrix with

$$\mathbf{a}(\theta_{\hat{n}}) = \left[1, e^{\left(-j\frac{2\pi\bar{b}}{\lambda}\sin(\theta_{\hat{n}})\right)}, \cdots, e^{\left(-j\frac{2\pi\bar{b}_{M-1}}{\lambda}\sin(\theta_{\hat{n}})\right)}\right]^T \tag{3}$$

denoting the steering vector, with the position of the first element set at the origin. The goal is to optimize the subarray spacing $\bar{\mathbf{s}}$ such that the RMSE of the DOA estimation is minimized under the given noise conditions.

Due to the presence of impulsive noise, it is necessary to preprocess the received data to mitigate its impact. Consequently, we employ the INEK technique, which has proven to be very robust against impulsive noise [17]. The $(\bar{i}, \bar{j})$th of INEK matrix is given by

$$\hat{R}_{ij} = \frac{1}{L}\sum_{l=1}^{L} z_i(l) z_j^*(l) \exp\left(-\eta |z_i(l) - \mu z_j^*(l)|\right) \tag{4}$$

$$\mathbf{z}(l) = \frac{\mathbf{B}(l)}{\max\{|B_1(l)|, |B_2(l)|, \cdots, |B_M(l)|\}} \tag{5}$$

where L denotes the number of snapshots, η a kernel constant within [0, 1], and μ a constant within [0, 2].

Further, perform eigenvalue decomposition on $\hat{\mathbf{R}}$, given by

$$\hat{\mathbf{R}} = \mathbf{U}_S \hat{\boldsymbol{\Sigma}}_S \mathbf{U}_S^H + \mathbf{U}_N \hat{\boldsymbol{\Sigma}}_N \mathbf{U}_N^H \tag{6}$$

where $\mathbf{U}_S$ and $\mathbf{U}_N$ are the signal and noise subspaces spanned by the eigenvectors corresponding to the N large eigenvalues and remaining small eigenvalues; $\hat{\boldsymbol{\Sigma}}_S$ and $\hat{\boldsymbol{\Sigma}}_N$ are the diagonal matrices formed by the corresponding N large eigenvalues and remaining small eigenvalues. Next, we construct the following spectral function

$$P(\theta) = \frac{1}{\mathbf{a}^H(\theta)\hat{\mathbf{U}}_N \mathbf{U}_N^H \mathbf{a}(\theta)} \tag{7}$$

Subsequently, using the spectral peak search method, we identify the N maxima of (7), which correspond to the estimated DOAs $\hat{\boldsymbol{\theta}} = [\hat{\theta}_1, \hat{\theta}_2, \cdots, \hat{\theta}_N]$ for the distributed array. Finally, the RMSE of the DOA estimates is computed to evaluate the

direction-finding performance of the distributed array under this layout serving as the objective function to be optimized in our proposed method, i.e.,

$$F(\bar{\mathbf{s}}) = \sqrt{\sum_{i=1}^{N} \frac{\left(\theta_i - \hat{\theta}_i\right)^2}{N}} \tag{8}$$

A smaller RMSE indicates better array performance. $\bar{\mathbf{s}}$ denotes a potential solution for the distributed array's subarray layout.

Upon defining the objective function for optimization, we propose a DQEFO algorithm in the next section to search for the optimal sub-array arrangement. This approach not only reduces the computational complexity of the optimization problem but also ensures the superiority of the resulting sub-array layout.

3. DOA ESTIMATION USING DQEFO-BASED DISTRIBUTED ARRAY OPTIMIZATION

3.1. DQEFO Algorithm

In the discrete quantum electromagnetic field optimization algorithm, we first assume the presence of K quantum electromagnetic particles in the electromagnetic field, each with a corresponding quantum position. The quantum position of the kth quantum electromagnetic particle at the tth iteration is denoted as

$$\mathbf{y}_k^t = [y_{k,1}^t, y_{k,2}^t, \cdots, y_{k,Q}^t] \tag{9}$$

where $0 \le y_{k,q}^t \le 1$. By measuring, we obtain the measurement position

$$\mathbf{x}_k^t = [x_{k,1}^t, x_{k,2}^t, \cdots, x_{k,Q}^t] \tag{10}$$

where $x_{k,q}^t \in \{0, 1\}$, $q = 1, 2, \cdots, Q$, with Q being the maximum dimension of the solution space.

Calculating the fitness function value and the local optimal position of the kth quantum electromagnetic particle until the tth iteration is denoted as

$$\mathbf{p}_k^t = [p_{k,1}^t, p_{k,2}^t, \cdots, p_{k,Q,}^t] \tag{11}$$

The global optimal position of the entire electromagnetic field until the tth iteration is denoted as

$$\mathbf{g}_k^t = [g_{k,1}^t, g_{k,2}^t, \cdots, g_{k,Q,}^t] \tag{12}$$

Based on the characteristics of the actual electromagnetic field and referencing the fitness values of the particles, the quantum electromagnetic particles in the field are divided into three polarities: positive, neutral, and negative, with proportions of $\hat{\beta}$, $\hat{\vartheta}$, and $\hat{\zeta}$, respectively. All electromagnetic particles update their positions using the following two quantum update strategies.

Strategy 1: Generate a random number $\delta_{k,q}$ uniformly distributed between [0, 1]. If $\delta_{k,q} < \rho$, ρ is the selection probability, then the qth quantum rotation angle of the kth quantum electromagnetic particle at the tth iteration is defined as

$$v_{k,q}^{t+1} = r_1(x_{\beta,q}^t - x_{k,q}^t) + r_2(p_{\sigma,q}^t - x_{k,q}^t) \tag{13}$$

If $\delta_{k,q} \ge \rho$, the corresponding quantum rotation angle is defined as

$$v_{k,q}^{t+1} = r_3(g_q^t - x_{k,q}^t) + \varphi r_4(x_{\beta,q}^t - x_{k,q}^t) - r_5(x_{\zeta,q}^t - x_{\vartheta,q}^t) \tag{14}$$

where r_1, r_2, r_3, r_4, and r_5 are random numbers uniformly distributed between [0, 1], φ is a scaling factor; $x_{\beta,q}^t$ is the qth dimension of the βth positively polarized particle in the tth iteration; $x_{\zeta,q}^t$ is the qth dimension of the ζth negatively polarized particle in the tth iteration; $x_{\vartheta,q}^t$ is the qth dimension of the ϑth neutrally polarized particle in the tth iteration; $p_{\sigma,q}^t$ is the qth dimension of the σth local optimal position in the tth iteration; and g_q^t is the qth dimension of the global optimal position in the$t$th iteration and $\mathbf{v}_k^{t+1} = [v_{k,1}^{t+1}, v_{k,2}^{t+1}, \cdots, v_{k,Q}^{t+1}]$, $q = 1, 2, \cdots, Q$.

Then update the quantum position of the electromagnetic particle as

$$y_{k,q}^{t+1} = \begin{cases} \sqrt{1 - (y_{k,q}^t)^2} & v_{k,q}^{t+1} = 0, \eta_{k,q}^{t+1} < c_1 \\ \left| y_{k,q}^t \times \cos v_{k,q}^{t+1} \right. & \\ \left. -\sqrt{1 - (y_{k,q}^t)^2} \times \sin v_{k,q}^{t+1} \right| & v_{k,q}^{t+1} \ne 0 \end{cases} \tag{15}$$

where $\eta_{k,q}^{t+1}$ is a random number uniformly distributed between [0, 1], and c_1 is the probability of flipping the qubit when the quantum rotation angle is 0, which is a constant within the range of $[0, 1/Q]$. Then, the position $x_{k,q}^t$ is obtained by measuring the quantum position, with the measurement equation given by

$$x_{k,q}^{t+1} = \begin{cases} 1, j_{k,q}^{t+1} > (y_{k,q}^{t+1})^2 \\ 0, j_{k,q}^{t+1} \le (y_{k,q}^{t+1})^2 \end{cases} \tag{16}$$

where $j_{k,q}^{t+1}$ is a uniformly distributed random number between [0, 1], $q = 1, 2, \cdots, Q$.

Strategy 2: Updating the quantum rotation angle again, the update formula for the qth dimension of the quantum rotation angle of the kth quantum electromagnetic particle is given by

$$v_{k,q}^{t+1} = u_1(b_q^t - x_{k,q}^t) + u_2(g_q^t - x_{k,q}^t) \tag{17}$$

where u_1 and u_2 are random numbers following a standard Gaussian distribution; $b_q^t = (1/K)\sum_{k=1}^{K} p_{k,q}^t$ represents the qth dimension of the mean value of K local optimal positions; $\mathbf{b}_k^{t+1} = [b_{k,1}^{t+1}, b_{k,2}^{t+1}, \cdots, b_{k,Q}^{t+1}]$, $q = 1, 2, \cdots, Q$. Then update the quantum position of the electromagnetic particle as

$$y_{k,q}^{t+1} = \begin{cases} \sqrt{1 - (y_{k,q}^t)^2} & v_{k,q}^{t+1} = 0, \tilde{\eta}_{k,q}^{t+1} < c_1 \\ \left| y_{k,q}^t \times \cos v_{k,q}^{t+1} \right. & \\ \left. -\sqrt{1 - (y_{k,q}^t)^2} \times \sin v_{k,q}^{t+1} \right| & v_{k,q}^{t+1} \ne 0 \end{cases} \tag{18}$$

where $\tilde{\eta}_{k,q}^{t+1}$ is a random number uniformly distributed between [0, 1], and the corresponding measurement equation is given by

$$x_{k,q}^{t+1} = \begin{cases} 1, \tilde{j}_{k,q}^{t+1} > (y_{k,q}^{t+1})^2 \\ 0, \tilde{j}_{k,q}^{t+1} \leq (y_{k,q}^{t+1})^2 \end{cases} \tag{19}$$

where $\tilde{j}_{k,q}^{t+1}$ is a uniformly distributed random number between [0, 1], $q = 1, 2, \cdots, Q$.

3.2. DQEFO-Based Distributed Array Optimization and DOA Estimation

In DQEFO, the quantum positions of the population are uniformly initialized in the range of [0, 1], and the fitness function is defined as

$$\bar{F}(\mathbf{x}_k^t) = \sqrt{\sum_{i=1}^{N} \frac{(\theta_i - \hat{\theta}_i)^2}{N}} \tag{20}$$

Note that the optimization parameter is an integer vector $\bar{\mathbf{s}} = [\bar{s}_1, \bar{s}_2, \cdots, \bar{s}_{Z-1}]$, while the potential solution, represented by the measurement position of the quantum electromagnetic particles in the DQEFO algorithm, is composed of Q-bit binary numbers. Therefore, a data conversion is necessary to achieve a one-to-one correspondence between the measurement position potential solution $\mathbf{x}_k^t$ and $\bar{\mathbf{s}}_k^t$. The conversion method is as follows: for the measurement position $\mathbf{x}_k^t = [x_{k,1}^t, x_{k,2}^t, \cdots, x_{k,Q}^t]$, each $Q/(Z-1)$ position is transformed into a decimal integer group, resulting in the $Z-1$ subarray layout structure potential solution $\bar{\mathbf{s}}_k^t = [\bar{s}_{k,1}^t, \bar{s}_{k,2}^t, \cdots, \bar{s}_{k,Z-1}^t]$.

Once the optimal subarray layout is obtained, we perform DOA estimation using INEK-based ML method [17] to obtain the optimal angular estimate for this array structure, given by

$$\hat{\boldsymbol{\theta}} = \arg\max_{\boldsymbol{\theta}} \operatorname{tr}\left(\mathbf{P}_A(\boldsymbol{\theta})\hat{\mathbf{R}}\right) \tag{21}$$

The steps of the proposed method are as follows:

Algorithm 1 DOA estimation using DQEFO-based distributed array optimization

1 Input: Distributed array system parameters and parameters for DOA Estimation;
2 Initialize: Parameters of DQEFO algorithm;
3 Let $t = 1$ //the first iteration;
4 Initialize the quantum electromagnetic particles, including their respective quantum positions and measured positions, and obtain a set of local optimal measured positions;
5 Transform the measured position of the electromagnetic particle into the subarray spacing vector, then evaluate the fitness function, and obtain the global optimal measurement position;
6 while $t \leq t_{\max}$ //$t_{\max}$ represents the maximum number of iterations
7 Update quantum positions using two strategies;
8 Calculate the fitness value of the updated electromagnetic particle;
9 Update the set of local optimal measurement positions;
10 Update the global optimal measurement position in a greedy manner;
11 Let $t = t + 1$;
12 end while
13 Transform the global optimal solution into the required subarray structure;
14 Output: Optimal subarray spacing vector;
15 Conduct DOA estimation using INEK-based ML method;
16 Output: DOA estimates.

4. SIMULATION RESULTS

The RMSE is used for performance evaluation, defined as

$$RMSE = \sqrt{\sum_{i=1}^{N}\sum_{o=1}^{E_r} \frac{\left(\theta_i - \hat{\theta}_{io}\right)^2}{NE_r}} \tag{22}$$

where $\hat{\theta}_{io}$ denotes the ith estimated DOA in the oth trial, and E_r is the number of simulation trials.

In addition, in the presence of impulsive noise, the generalized signal-to-noise ratio (GSNR) is used instead of the SNR,

$$GSNR = 10\lg\left\{\frac{E[\|\mathbf{s}(t)\|^2]}{\gamma^{\alpha}}\right\} \tag{23}$$

where $E[\cdot]$ and $\|\cdot\|$ stand for the expectation and the Euclidean norm.

In the simulations, $M = 100$, $G = 10$, $Z = 10$, $\hat{d} = \lambda/2$. For the DQEFO algorithm $K = 40$, $Q = 72$, $T = 300$, $\hat{\beta} = 0.1$, $\hat{\vartheta} = 0.5$, $\hat{\zeta} = 0.4$, $\rho = 0.2$, and $\varphi = (\sqrt{5}+1)/2$ [17]. The number of auxiliary sources is $N = 4$, with incident angles $\theta_1 = 55.74^\circ$, $\theta_2 = 15.64^\circ$, $\theta_3 = 5.76^\circ$, and $\theta_4 = -30.5^\circ$. The characteristic exponent is $\alpha = 1.5$. The generalized signal-GSNR $= 3$ dB. The step size of spectral peak search is 0.1°, $L = 20$, η=0.5, μ=0.35 [17].

Under the aforementioned parameter settings, the optimal sub-array layout structure of the distributed system is obtained by selecting the best value through multiple tests. The inter-sub-array spacing is determined as follows

$$D = [169\hat{d}, 108\hat{d}, 4\hat{d}, 70\hat{d}, 92\hat{d}, 56\hat{d}, 94\hat{d}, 54\hat{d}, 112\hat{d}] \tag{24}$$

To further validate the superiority of the proposed array structure, we tested the DOA estimation performance under various adverse conditions, such as limited snapshots, impulsive noise, and low GSNR scenarios. Employed with the obtained optimal array structure, our method using INEK-based ML method for DOA estimation (denoted as DQEFO-INEKML), which is compared to the classical MUSIC method with a spectral peak search step size of 0.1° (denoted as DQEFO-MUSIC). Additionally, we compare the proposed method with conventional equally spaced uniform arrays using MUSIC method, including distributed arrays with sub-array spacings of $10\hat{d}$, $20\hat{d}$, and $50\hat{d}$ (denoted as 10-fold spacing-MUSIC, 20-fold spacing-MUSIC, and 50-fold spacing-MUSIC, respectively), and a uniform linear array (denoted as ULA-MUSIC). For all scenarios, $E_r = 500$.

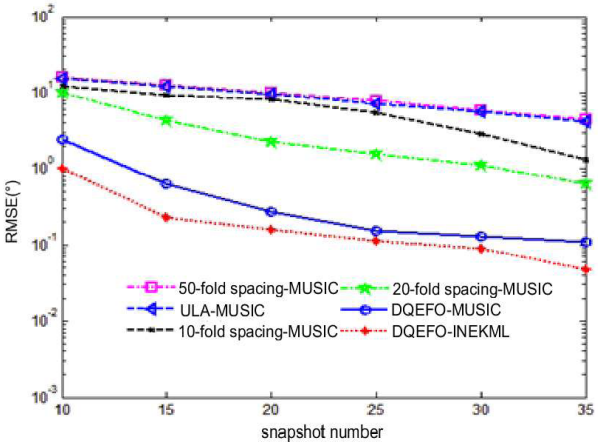

FIGURE 2. RMSE curves with the variation of snapshot number under different array structures.

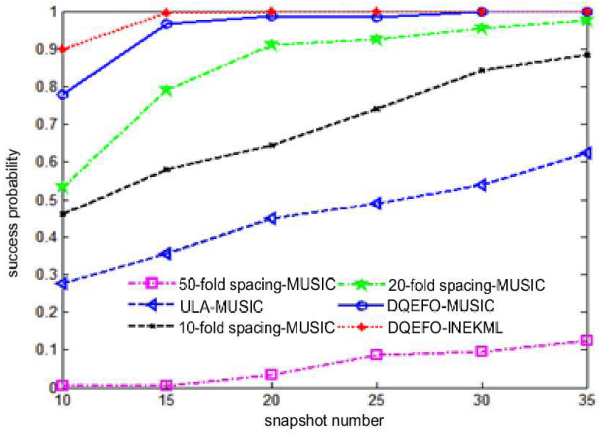

FIGURE 3. Success probability curves with the variation of snapshot number under different array structures.

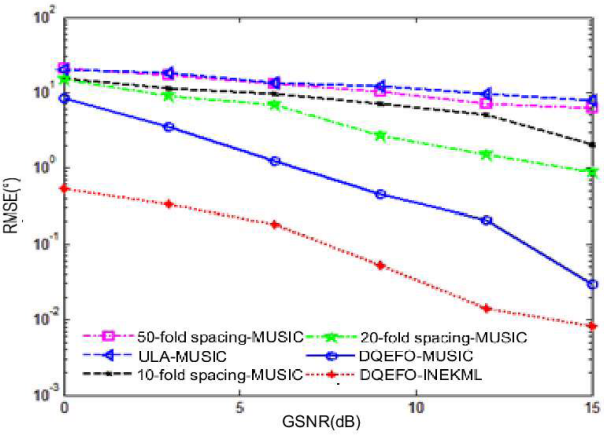

FIGURE 4. RMSE curves with the variation of GSNR under different array structures.

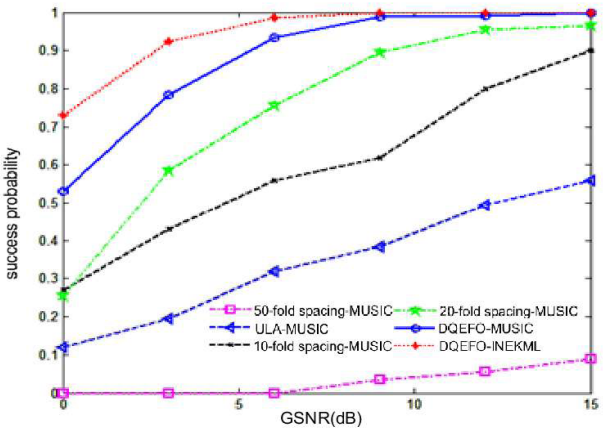

FIGURE 5. Success probability curves with the variation of GSNR under different array structures.

Scenario 1: Consider three independent sources with incident directions of $\theta_1 = 55.74^{\circ}$, $\theta_2 = 15.64^{\circ}$, and $\theta_3 = -30.5^{\circ}$. Fig. 2 and Fig. 3 show the impact of the number of snapshots on the RMSE and success probability of different array structures under impulsive noise with GSNR $= 10$ dB and $\alpha = 1.5$. The estimation is deemed successful if the error between the estimated value and actual value is less than 2.5°.

From the figures, it is evident that under a low number of snapshots, the proposed method based on the optimized distributed array demonstrates superior direction-finding accuracy and robustness compared to other array structures. This indicates a clear advantage in DOA estimation and shows that the proposed layout structure is capable of adapting to applications with a low number of snapshots, overcoming the limitations of existing layout structures.

Figures 4 and 5 illustrate the impact of GSNR on the RMSE and success probability of different array structures under impulsive noise, with a snapshot number of 20. From the figures, it is evident that under conditions of low snapshots and low GSNR, the proposed array structure significantly outperforms other structures in DOA estimation performance. The proposed DQEFO-INEKML method shows a substantial improvement in DOA estimation performance as the GSNR conditions improve, demonstrating a clear and significant advantage.

Scenario 2: To validate the direction-finding performance of the proposed array structure under different numbers of sources, we first consider four independent sources with incident angles of $\theta_1 = 55.74^{\circ}$, $\theta_2 = 15.64^{\circ}$, $\theta_3 = 5.76^{\circ}$, and $\theta_4 = -30.5^{\circ}$. Fig. 6 presents the impact of snapshot numbers on RMSE for different array structures under impulsive noise with GSNR $= 10$ dB and $\alpha = 1.2$. The results demonstrate that under conditions of impulsive noise and low snapshots, the proposed array structure and direction-finding method exhibit significant superiority. The RMSE of the proposed distributed array optimization-based direction-finding method is substantially lower than that of other methods.

Figure 7 shows the impact of snapshot numbers on success probability. It can be observed that, under low snapshot conditions, the direction-finding method based on the proposed array structure achieves a higher estimation success probability than

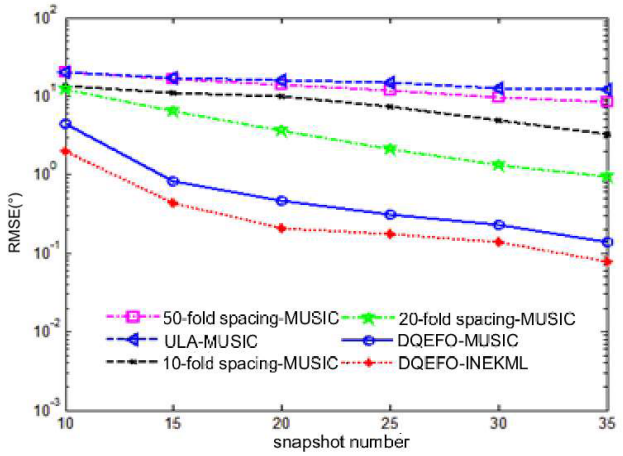

FIGURE 6. RMSE curves with the variation of snapshot number under different array structures.

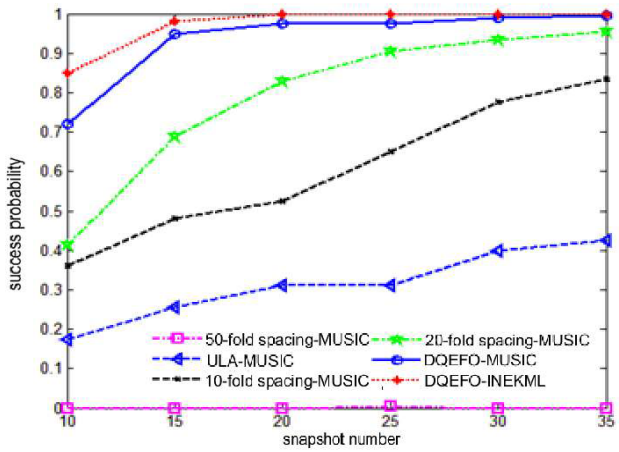

FIGURE 7. Success probability curves with the variation of snapshot number under different array structures.

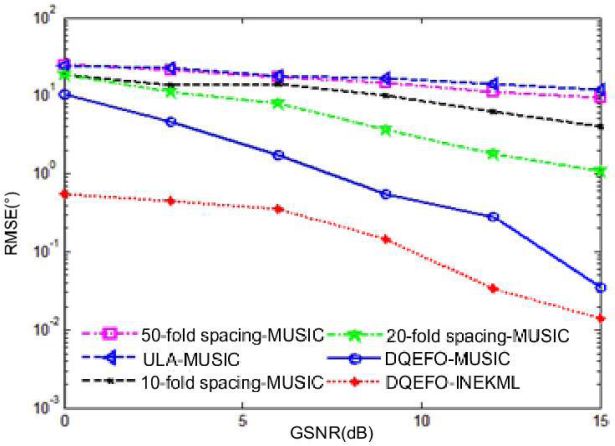

FIGURE 8. RMSE curves with the variation of GSNR under different array structures.

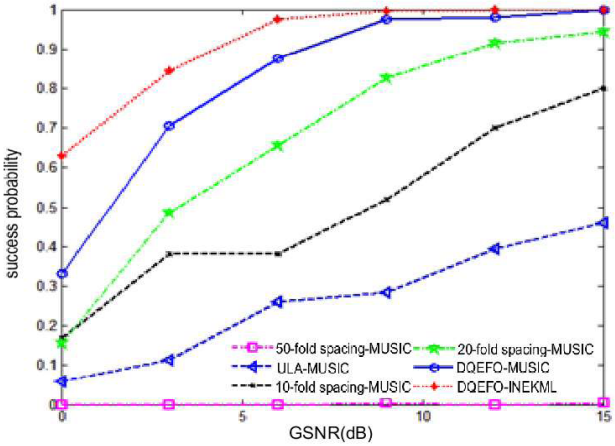

FIGURE 9. Success probability curves with the variation of GSNR under different array structures.

other structures. The proposed distributed array optimization-based direction-finding method exhibits superior robustness and performance. The simulation results indicate that the proposed layout structure can adapt to low snapshot application conditions, overcoming the limitations of existing array layout structures.

Figures 8 and 9 illustrate the impacts of GSNR on RMSE and success probability, with a snapshot number of 20. The results show that the proposed DOA estimation method based on distributed array optimization exhibits superior angular accuracy and a higher angle estimation success probability compared to other array structures. As the GSNR increases, the performance of the proposed method improves significantly, demonstrating notable advantages in DOA estimation.

5. CONCLUSIONS

This paper introduces a novel DQEFO algorithm, designed to effectively solve discrete optimization problems. Addressing the issue of suboptimal accuracy and severe performance degradation under adverse conditions in existing distributed array methods, which often utilize uniform array configurations, we construct an objective function based on the RMSE of the estimated DOA of sources. The DQEFO algorithm is then employed to solve this objective function, resulting in the optimal sub-array configuration. Utilizing this optimized array structure, we apply the INEK-ML method for DOA estimation. Comparative simulations across different array structures demonstrate that the proposed method effectively achieves accurate DOA estimates even in the presence of impulsive noise, low snapshots, and low GSNR. However, the designed DQEFO algorithm employs serial evolution during execution. Without a high-speed parallel executor, the runtime will increase with the population size. Additionally, it may encounter issues with slow convergence speed and poor convergence accuracy when handling large-scale integer optimization problems, to be explored in our future research focus.

REFERENCES

[1] Heimiller, R. C., J. E. B. Tomlinson, and P. G., "Distributed array radar," *IEEE Transactions on Aerospace and Electronic Systems*, Vol. 19, No. 6, 831–839, Nov. 1983.

[2] Lou, Y., X. Qu, D. Wang, and J. Cheng, "Direction-of-arrival estimation for nested acoustic vector-sensor arrays using quaternions," *IEEE Transactions on Geoscience and Remote Sensing*, Vol. 61, 1–14, Article Sequence Number 4 204 714, 2023.

[3] Liu, Y., H. Gao, Y. Du, M. Chen, and R. Sun, "Low-complexity doa estimation for coherently distributed sources with gain-phase errors in massive mimo systems," *IEEE Transactions on Vehicular Technology*, Vol. 73, No. 6, 7939–7948, June 2024.

[4] Zhang, X., Z. Zheng, W.-Q. Wang, and H. C. So, "Joint dod and doa estimation of coherent targets for coprime mimo radar," *IEEE Transactions on Signal Processing*, Vol. 71, 1408–1420, 2023.

[5] Liu, Y., H. Gao, Y. Du, M. Chen, and R. Sun, "DOA estimation for mixed circular and noncircular coherently distributed sources under impulsive noise," *IEEE Transactions on Aerospace and Electronic Systems*, 1–16, 2024.

[6] Liao, B., Z. Zhang, and S. C. Chan, "Chapter 5 - subspace tracking for time-varying direction-of-arrival estimation with sensor arrays," *IoT and Spacecraft Informatics*, 129–155, K. L. Yung, Andrew W. H. Ip, Fatos Xhafa, K. K. Tseng (eds.), Elsevier Aerospace Engineering Series, 2022. [Online]. Available: https://www.sciencedirect.com/science/article/pii/B9780128210512000118

[7] Nurbas, E., E. Onat, and T. E. Tuncer, "Collaborative direction of arrival estimation by using alternating direction method of multipliers in distributed sensor array networks employing sparse bayesian learning framework," *Digital Signal Processing*, Vol. 130, No. 10, 103739, Oct. 2022.

[8] Sun, J., P. Li, J. Mao, M. Yang, D. Shao, Y. Chen, J. Li, and K. Wang, "Performance analysis of beamforming algorithm based on compressed sensing," *Applied Acoustics*, Vol. 198, No. 2, 108987, Sep. 2022.

[9] Liang, L., Y. Shi, Y. Shi, Z. Bai, and W. He, "Two-dimensional doa estimation method of acoustic vector sensor array based on sparse recovery," *Digital Signal Processing*, Vol. 120, No. 5, 103294, Jan. 2022.

[10] Wang, P., H. Yang, and Z. Ye, "1-bit direction of arrival estimation via improved complex-valued binary iterative hard thresholding," *Digital Signal Processing*, Vol. 120, No. C, 103265, Jan. 2022.

[11] Geng, L., J. Zhou, Z. Sun, and J. Tang, "Compressive hard thresholding pursuit algorithm for sparse signal recovery," *Aims Mathematics*, Vol. 7, No. 9, 16 811–16 831, 2022.

[12] Shen, Y., C. Yu, Y. Shen, and S. Li, "On sparse recovery algorithms in unions of orthonormal basest," *Journal of Approximation Theory*, Vol. 289, 105886, May 2023.

[13] Zhang, J., X. Ren, J. Li, Y. Liu, and W. Zhang, "DOA estimation of non-circular signals based on iterative soft thresholding algorithm," *International Journal of RF and Microwave Computer-aided Engineering*, Vol. 32, No. 2, 23391, Nov. 2022.

[14] Zhang, J., P. Chu, and B. Liao, "Doa estimation in impulsive noise based on fista algorithm," *Remote Sensing*, Vol. 15, No. 3, 565, Feb. 2023.

[15] Patel, S. and A. Vaish, "An efficient optimization of measurement matrix for compressive sensing," *Journal of Visual Communication and Image Representation*, Vol. 95, 103904, Sep. 2023.

[16] Zhao, Y. and Z. Luo, "Improved rip-based bounds for guaranteed performance of two compressed sensing algorithms," *Science China-mathematics*, Vol. 66, No. 5, 1123–1140, May 2023.

[17] Yanan, D., G. Hongyuan, and C. Menghan, "Direction of arrival estimation method based on quantum electromagnetic field optimization in the impulse noise," *Journal of Systems Engineering and Electronics*, Vol. 32, No. 3, 527–537, Jun. 2021.

[18] Abedinpourshotorban, H., S. M. Shamsuddin, Z. Beheshti, and D. N. A. Jawawi, "Electromagnetic field optimization: A physics-inspired metaheuristic optimization algorithm," *Swarm and Evolutionary Computation*, Vol. 26, 8–22, Feb. 2016.